The Response of MSTd Neurons to Perturbations in Target Motion During Ongoing Smooth-Pursuit Eye Movements

Seiji Ono, Lukas Brostek, Ulrich Nuding, Stefan Glasauer, Ulrich Büttner and Michael J. Mustari

J Neurophysiol 103:519-530, 2010. First published 18 November 2009; doi:10.1152/jn.00563.2009

J Neurophysiol 103: 519–530, 2010.
First published November 18, 2009; doi:10.1152/jn.00563.2009.

The Response of MSTd Neurons to Perturbations in Target Motion During Ongoing Smooth-Pursuit Eye Movements

Seiji Ono,[2] Lukas Brostek,[3] Ulrich Nuding,[3] Stefan Glasauer,[3] Ulrich Büttner,[3] and Michael J. Mustari[1]

[1]*Washington National Primate Research Center, University of Washington, Seattle, Washington;* [2]*Yerkes National Primate Research Center, Emory University, Atlanta, Georgia; and* [3]*Bernstein Center for Computational Neuroscience, University of Munich, Munich, Germany*

Submitted 1 July 2009; accepted in final form 10 November 2009

Ono S, Brostek L, Nuding U, Glasauer S, Büttner U, Mustari MJ. The response of MSTd neurons to perturbations in target motion during ongoing smooth-pursuit eye movements. *J Neurophysiol* 103: 519–530, 2010. First published November 18, 2009; doi:10.1152/jn.00563.2009. Several regions of the brain are involved in smooth-pursuit eye movement (SPEM) control, including the cortical areas MST (medial superior temporal) and FEF (frontal eye field). It has been shown that the eye-movement responses to a brief perturbation of the visual target during ongoing pursuit increases with higher pursuit velocities. To further investigate the underlying neuronal mechanism of this nonlinear dynamic gain control and the contributions of different cortical areas to it, we recorded from MSTd (dorsal division of the MST area) neurons in behaving monkeys (*Macaca mulatta*) during step-ramp SPEM (5–20°/s) with and without superimposed target perturbation (one cycle, 5 Hz, ±10°/s). Smooth-pursuit–related MSTd neurons started to increase their activity on average 127 ms after eye-movement onset. Target perturbation consistently led to larger eye-movement responses and decreasing latencies with increasing ramp velocities, as predicted by dynamic gain control. For 36% of the smooth-pursuit–related MSTd neurons the eye-movement perturbation was accompanied by detectable changes in neuronal activity with a latency of 102 ms, with respect to the eye-movement response. The remaining smooth-pursuit–related MSTd neurons (64%) did not reflect the eye-movement perturbation. For the large majority of cases this finding could be predicted by the dynamic properties of the step-ramp responses. Almost all these MSTd neurons had large visual receptive fields responding to motion in preferred directions opposite to the optimal SPEM stimulus. Based on these findings it is unlikely that MSTd plays a major role for dynamic gain control and initiation of the perturbation response. However, neurons in MSTd could still participate in SPEM maintenance. Due to their visual field properties they could also play a role in other functions such as self-motion perception.

INTRODUCTION

Moving visual stimuli can induce slow tracking eye movements. For small objects these are called smooth-pursuit eye movements (SPEMs). They are used to keep the image of the moving object on or near the fovea where visual acuity is best. SPEMs are produced by volitional effort and depend on motivation, attention, and target motion.

SPEMs can reach velocities up to ≥60°/s (for review see Krauzlis 2004; Leigh and Zee 2006). In the laboratory, SPEMs are often investigated with a step-ramp paradigm (Rashbass 1961). In this paradigm, the monkey fixates a stationary target, which after a delay is replaced by a target located slightly eccentrically that moves toward the fovea at a constant speed. It allows SPEMs to be elicited at short latency (100–140 ms) without contamination by initial saccades.

In recent years it was shown that during ongoing constant-velocity SPEMs, brief perturbations of target motion exhibit a velocity-dependent effect on eye velocity. Typically a short-duration (<200 ms) single cycle (5–10 Hz) of sinusoidal motion is added to the ongoing target motion, resulting in a corresponding perturbation of eye motion. The eye motion response depends on current SPEM speed in both humans (Churchland and Lisberger 2002) and monkeys (Churchland and Lisberger 2005b), even when the same perturbing stimulus motion is applied. While fixating a stationary target, perturbation responses are still produced but at a lower gain (Schwartz and Lisberger 1994). This nonlinear response is thought to reveal an underlying dynamic gain control mechanism in SPEM (Churchland and Lisberger 2005b; Nuding et al. 2008). Even though the neural mechanisms and regions involved in dynamic gain control are not completely understood, recent studies point toward cortical areas as being the main site of smooth-pursuit gain control (Nuding et al. 2008; Tanaka and Lisberger 2001).

From single-unit and lesion studies it is known that frontal lobe and parietal–occipital lobe structures play complementary roles in SPEM (Krauzlis 2004). These areas include the middle temporal (MT) and medial superior temporal (MST) areas in the parietooccipital region and the frontal eye field (FEF) cortex. These cortical areas are reciprocally connected (Tusa and Ungerleider 1988) and also send projections to the brain stem (Distler et al. 2002). Area MT, which has extensive connections with MST, is well known to play a role in visual motion processing, including foveal and parafoveal visual motion appropriate for SPEMs (Maunsell and Van Essen 1983). MST is divided into several subregions, including dorsal (MSTd), lateral (MSTl), and ventral (MSTv), with different functional properties. Lesions of MST cause deficits in SPEM when the subject tracks a target moving toward the lesioned side (Newsome et al. 1988).

Early single-unit recording studies demonstrated that during SPEM neurons in MSTd and MSTl show strong modulation that was often due to an extraretinal signal (Newsome et al. 1988). The extraretinal origin was revealed by briefly (100–400 ms) extinguishing the target spot during maintained SPEM. In this target blink condition, well-trained monkeys maintain most of their smooth-pursuit eye velocity (e.g., Ono

Address for reprint requests and other correspondence: M. J. Mustari, Washington National Primate Research Center, University of Washington, Seattle, WA 98195 (E-mail: mmustar@wanprc.org).

and Mustari 2006), MSTd and some MSTl neurons continue to discharge (Newsome et al. 1988), but MT neurons do not.

Neurons in MSTd have large visual receptive fields (>14°) that can include both contralateral, foveal, and ipsilateral visual field components (Churchland and Lisberger 2005b). The large-field visual and smooth-pursuit response components of MSTd neurons generally have opposing direction preferences (Komatsu and Wurtz 1988). Based on the interaction of the visual and extraretinal components it has been argued that MSTd might be a critical structure for self-motion perception (Shenoy et al. 2002).

During step-ramp testing a large proportion of MSTd neurons begin firing only 50–100 ms after pursuit onset (Newsome et al. 1988). Only a small subset of MSTd neurons has short-latency responses starting as much as 100 ms before smooth-pursuit initiation (Newsome et al. 1988). This early response component might be due to retinal image motion of the target (Ilg and Thier 2003).

We have demonstrated in earlier studies that MST projects to the dorsolateral pontine nuclei (DLPN) (Distler et al. 2002). Similarly, the FEF projects to the nucleus reticularis tegmenti pontis (NRTP) (Ono and Mustari 2009). Both DLPN (Mustari et al. 1988; Thier et al. 1988) and NRTP (Ono et al. 2004; Suzuki et al. 2003) are known to play a role in SPEM. The DLPN and NRTP have been shown in anatomical studies to project to mostly different regions of the cerebellum including the floccular complex and vermis. In turn, the floccular complex and vermis deliver signals important for SPEM through the vestibular nuclei and caudal fastigial nuclei, respectively (Büttner and Büttner-Ennever 2006). Moreover, there is now strong evidence for a feedback loop via the thalamus back to the cortex (Tanaka 2005), which might carry an efference copy of SPEM commands (Nuding et al. 2008).

The goal of our studies was to determine the potential role of MSTd neurons in the control of visually induced perturbation responses during SPEM. To accomplish this, we recorded single-unit activity in MSTd of the alert behaving monkey during a step-ramp paradigm, which included a target perturbation task. We found that a minority of MSTd neurons was modulated during the perturbation task, with neuronal response onsets about 100 ms after the eye movement caused by the perturbation. To contrast these responses a few neurons were also tested during eye movements induced by large-field visual motion. The preferred neuronal response was in the direction opposite to the optimal SPEM response. Under these conditions virtually all neurons responded before the step-ramp and perturbation-induced eye movements. The results indicate that MSTd neurons probably do not play a major role in the initiation of the perturbation responses during SPEM; however, they could contribute to SPEM control during maintained tracking.

METHODS

Three monkeys (*Macaca mulatta*, 5–7 kg), born in captivity at the Yerkes National Primate Research Center (Atlanta, GA), were prepared for chronic eye-movement and single-unit recordings. All surgical procedures were performed in compliance with National Institutes of Health *Guide for the Care and Use of Laboratory Animals* and protocols were reviewed and approved by the Institutional Animal Care and Use Committee at Emory University. Surgical procedures were performed in a dedicated facility using aseptic techniques under isoflurane anesthesia (1.25–2.5%). Vital signs including blood pressure, heart rate, blood oxygenation, body temperature, and CO_2 in expired air were monitored with a Surgivet instrument (Waukesha, WI) and maintained within normal physiological limits. Postsurgical analgesia (buprenorphine, 0.01 mg/kg, administered intramuscularly [im]) and antiinflammatory (banamine, 1.0 mg/kg, im) treatment were delivered every 6 h for several days, as indicated. To permit single-unit recording, we used stereotaxic methods to implant a titanium head-stabilization post and a titanium recording chamber (Crist Instrument, Hagerstown, MD) over MST cortex (posterior, 5 mm; lateral, 15 mm). In the same surgery, a scleral search coil for measuring eye movements (Fuchs and Robinson 1966) was implanted underneath the conjunctiva of one eye using the technique of Judge et al. (1980).

Behavioral paradigms

During the experiments monkeys were seated in a primate chair (Crist Instrument) with their head fixed in the horizontal stereotaxic plane in a completely dark room to which they were customized. The room was sealed with darkroom tape and light traps to ensure no ambient light entered the room. This was verified by having a trained observer sit in the room for 30 min in complete darkness and attempt to find light leaks. Power to visual stimulus projector bulbs and to the laser diode, which provides the tracking target, were extinguished during blink testing. Neurons in MSTd were tested during smooth-pursuit and visual motion. All visual stimuli were rear-projected onto a tangent screen (Stewart Film Screen, Torrance, CA) at 57-cm distance. Stimuli were delivered using computer-controlled two-axis mirror galvanometers (General Scanning, Watertown, MA) and appropriate optics and hardware. Stimulus motion was controlled with custom LabVIEW software and National Instruments hardware (Austin, TX).

Localization of MSTd

We verified that our neurons were located in MSTd by functional (e.g., SPEM response continues during a target blink and large visual receptive fields), histological, and magnetic resonance imaging (MRI; T1-weighted, fast spin-echo; Siemens, 3-T magnet) criteria. Structural MRI was obtained from both monkeys while they were under surgical levels of inhalation anesthesia (described earlier). We confirmed the location of our recording sites histologically in one of the monkeys; the other monkeys are still being used in other studies. At the conclusion of our recording experiments, the first monkey was deeply anesthetized and perfused with physiological saline followed by 4% paraformaldehyde, as described in detail elsewhere (Mustari et al. 1994). Frozen sections were cut at 50 μm and every section was mounted on microscope slides and stained for Nissl substance to allow histological reconstruction of representative electrode tracks.

Visual stimuli

We searched for units in MSTd that were modulated during smooth-pursuit or visual motion in the frontal plane. We used either circular motion of a large-field visual stimulus or motion in eight cardinal directions, separated by 45° to determine neuronal direction preference. Visual stimuli were either large-field (35 × 35°) random dot patterns, small-field (5 × 5°) random dot patterns, or small-diameter (2°) spots. Random-dot patterns had light and dark contours with a mean luminance of 100 cd/m^2. Contrast of the light and dark contours was set at 50%. Circular motion was produced by driving the horizontal and vertical galvanometers 90° out of phase (±5–10°; 0.25–1.0 Hz). This circular motion stimulus produces constant-speed motion of all scene components across the full extent of the pattern. Smooth-pursuit direction preference was tested as using either circular motion (±10°; 0.25–0.5 Hz) or motion along eight cardinal directions

(U, up; D, down; L, left; R, right and the oblique directions: UL, UR, DL, DR) of a small-diameter (0.2°) target spot. The target was a rear-projected red spot produced with a light-emitting diode laser (Melles Griot, Rochester, NY). We maintained the target 1.0 log unit above the dark background, as measured with calibrated neutral density filters (Melles Griot). The optimal responses for smooth-pursuit tracking and large-field visual stimulation during fixation were usually in opposite directions. Except for the visual stimuli the monkey was in complete darkness. The following stimulus conditions were applied.

1) SPEM. The laser spot first stepped away from the center position and then moved at constant velocities from 5 to 20°/s in the preferred direction. The initial step was arranged so that the target crossed the center position after 130 ms. The constant-velocity part lasted 1,500–1,800 ms.

2) Large-field (LF) visual motion response. The monkey fixated a small target spot located at the center of gaze. The target was turned off coincident with the start of LF stimulus motion at constant velocity (5–20°/s) for 2,000 ms. This stimulus consistently leads to following eye movements (optokinetic response [OKR]).

3) Perturbation. During both SPEM and LF stimulation a visual perturbation consisting of one sinusoidal cycle (5 Hz, ±10°/s), with the first half-cycle increasing the stimulus velocity (peak-first perturbation; Churchland and Lisberger 2002), was introduced during the constant-velocity phase (600–800 ms after stimulus onset).

4) Blinking. Extraretinal modulation of neuronal response during SPEM was tested by blinking the target during ongoing pursuit for 100–200 ms. Trials with and without blinking were randomly interleaved (Ono and Mustari 2006). During the blink all visual stimuli were extinguished, leaving the monkey in complete darkness.

Visual receptive fields

Visual receptive fields (RFs) of neurons were mapped by moving a probe stimulus in the preferred and antipreferred directions at regularly spaced eccentricities across the visual field. The probe stimulus for RF mapping was a white rectangle (2 × 2°) oscillating at 0.5–3 Hz (±1°). RF size was taken as the area in which the neuron was modulated by the oscillating stimulus. Responses of our MSTd neurons were in agreement with known discharge properties of MSTd neurons (Komatsu and Wurtz 1988). Receptive fields were large and had their center in the contralateral hemifield. For most neurons RF size exceeded 30° and for many neurons it was >60°. None of the neurons had RFs <15° and they were not restricted to the central 15° around the fovea, as might be expected for other regions of MST (e.g., MSTl). Some neurons extended their RF into the ipsilateral hemifield, but generally not >20°. Larger extensions into the ipsilateral hemifield were always combined with increasing RF sizes. For 63% of the neurons the RF included the fovea. There was no difference in RF sizes for neighboring visual only and visual-smooth pursuit neurons.

Data collection

Eye movements were detected with standard electromagnetic methods using scleral search coils (Fuchs and Robinson 1966) and precision hardware (CNC Electronics, Seattle, WA). For calibration the monkey was required to fixate stationary targets at known eccentricities. Monkeys were rewarded with juice for maintaining fixation within a window of ±1.5°. Single-unit activity was recorded from neurons in MSTd using customized epoxy-coated tungsten microelectrodes (FHC, Bowdoin, ME) with an impedance of 1–3 MΩ. Single-unit action potentials were detected with either a hardware window discriminator (Bak Electronics, Mount Airy, MD) or template-matching algorithm (Alpha-Omega, Alpharetta, GA) and were registered at high precision as an event mark in our data-acquisition system (CED Power 1401, Cambridge Electronic Design, Cambridge, UK). Eye and target position feedback signals were processed with antialiasing filters at 200 Hz using six-pole Bessel filters before digitization at 1 kHz with 16-bit precision.

Data analysis

The recorded eye position traces were filtered with a Gaussian low-pass (cutoff frequency: 10 Hz) and three-point differentiated to obtain the velocity traces. Saccades were detected and removed with a slow-phase estimation algorithm as described previously (Ladda et al. 2007). Briefly, an estimate of the slow-phase component (SPC) was initialized to zero and iteratively improved in each step. The difference between the actual eye velocity trace and the current SPC served as an estimate of the fast-phase component (FPC). When the FPC exceeded a threshold (100°/s in the first step, 20°/s in the second step), a saccade was detected. The SPC was then computed by linear interpolation of the eye velocity across saccades and subsequent filtering with a Gaussian low-pass (cutoff frequency: 1 Hz in the first step, 10 Hz in the second step). Neuronal response was represented as a spike density function that was generated by convolving spike times with a 15-ms Gaussian function. Eye-movement and spike density functions corresponding to each trial were extracted and averaged over corresponding conditions.

To determine the eye-movement onset latency (EMOL) (Fig. 1), the mean and SD of the eye velocity during the initial fixation period were calculated. The point in time at which the eye velocity trace crosses the threshold of this mean + 3SD yields the EMOL, relative to target step-ramp onset ($t = 0$). The perturbation response latency (PRL), which describes the delay of the ocular response to target perturbation, was determined by the maximum of eye velocity in a time interval ≤400 ms after target perturbation. The difference of this maximum to the subsequent minimum of eye velocity yields the perturbation response modulation (PRM). For statistical assessment of these parameters, outliers deviating >3SD from the mean response were removed.

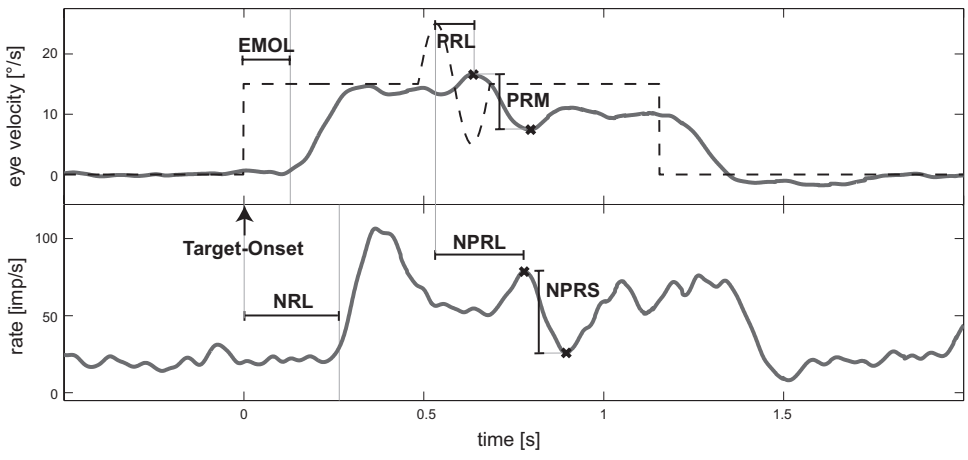

FIG. 1. Eye velocity (*A*) and neuronal parameters (*B*) measured. *A*: EMOL, eye-movement onset latency; PRL, perturbation response latency; PRM, perturbation response modulation. *B*: NRL, neuronal response latency; NPRL, neuronal perturbation response latency; NPRS, neuronal perturbation response sensitivity. Dashed line in *A* marks target velocity.

The neuronal response latency (NRL) denominates the delay of the increase in neural activity after target step-ramp onset. It was determined by the time when the response exceeds the mean + 3SD of the initial activity. The neuronal response sensitivity is the ratio of the mean spike density in a time interval between 500 and 600 ms after target step-ramp onset minus the mean initial spike density during fixation divided by the mean eye velocity in that time interval.

In the analysis associated with a blinking target the neuronal activity was compared with control trials without a blink. The blink response latency was defined as the point of minimal eye velocity in a period ≤400 ms after the start of blink. The time interval for determination of the response ratio consisted of a 200-ms period around this latency plus the neuronal latency with respect to the eye movements.

Data analysis of neuronal perturbation response

To decide whether a neuronal response shows modulation to a target perturbation, a confidence region was defined as a 3SD value around the Gaussian low-pass filtered (cutoff frequency: 2 Hz) spike density function of the control trials. When the spike density during the perturbation trials exceeded this confidence region in a time interval ≤550 ms after start of target perturbation, the neuronal response was declared to show a perturbation response.

If present, the delay of a neuronal modulation response to the perturbation of the visual target stimulus is described by the neuronal perturbation response latency (NPRL) (Fig. 1). It was determined by the maximum of spike density in a time interval ≤350 ms after target perturbation. The neuronal perturbation response sensitivity determines the ratio of the difference between this maximum and the subsequent minimum of spike density divided by twice the amplitude of the target perturbation.

We further analyzed whether a detectable perturbation response would be expected from the data by predicting the perturbation response based on the control trials. We first fitted a linear regression model with the regressor variables eye velocity (v) and eye acceleration (a) to the spike density function (sdf) of each neuron, according to

$$\text{sdf} = \beta_0 + \beta_1 \text{v} + \beta_2 \text{a}$$

Trial mean values were used for each target velocity from 500 ms before target onset until target offset. The lag of the neuronal response with respect to eye movement (NRL − EMOL) was taken into account by varying the delay in steps of 1 ms and searching for the best fit (maximal R^2). Using this model, we then predicted the neuronal response of the perturbation trials based on eye velocity and eye acceleration of these trials. The predicted response was then entered into the perturbation analysis described in the preceding paragraph. Thus neurons could fall in four classes (data responsive or not responsive; prediction responsive or not responsive), depending on whether a perturbation response was expected from the control responses.

RESULTS

In general, the majority (65%) of neurons encountered in the MSTd region responded only to visual motion. They will not be considered in the following text. For the present study, only SPEM-related MSTd neurons were included (n = 61). They were recorded in the right hemisphere of three monkeys (HZ, n = 48; UJ, n = 7; OY, n = 6 neurons) and were optimally modulated during SPEM in a preferred direction. Fifty-five of those also responded to visual motion, the remaining six only during SPEM. Generally, the preferred direction for visual motion and smooth pursuit was in opposite directions as reported previously (Newsome et al. 1988). All neurons were spontaneously active with a low and irregular firing rate.

SPEM perturbation responses

EYE MOVEMENTS. The perturbation (5 Hz, ±10°/s) during ongoing pursuit led in all instances to a change in eye velocity (Figs. 1, 2, and 3). We interleaved perturbation and normal step-ramp trials to prevent the monkey from anticipating a perturbation event. There was a tendency that trials with

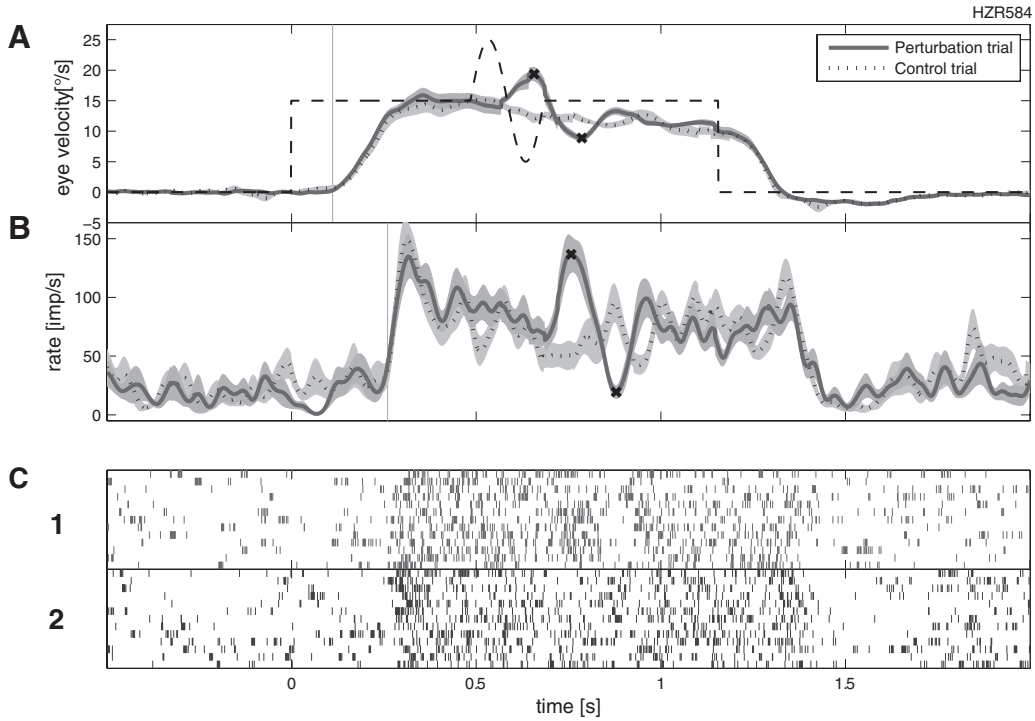

FIG. 2. MSTd (dorsal division of the medial superior temporal area) neuron during step-ramp smooth-pursuit eye movement (SPEM) and target perturbation. *A*: target and eye velocity. *B*: averaged neuronal activity from the individual traces shown in *C*. Continuous lines and *C1* refer to perturbation trials, dotted lines and *C2* to controls. Gray areas in *A* and *B* indicate SD of eye velocity and neuronal activity, respectively. Step-ramp stimulation leads to SPEM, followed by an increase in neuronal activity. The initial neuronal acceleration increase is followed by a constant velocity component. The perturbation (one cycle 5 Hz, ±10°/s) during the step-ramp stimulation leads to eye velocity changes and is also followed by a modulation of neuronal activity. Maximum and minimum of the eye and the neuronal perturbation response are marked by the analysis algorithm (METHODS), onset of SPEM (EMOL), and neuronal activity increase (NRL) (gray vertical line) as well. Time refers to stimulus onset.

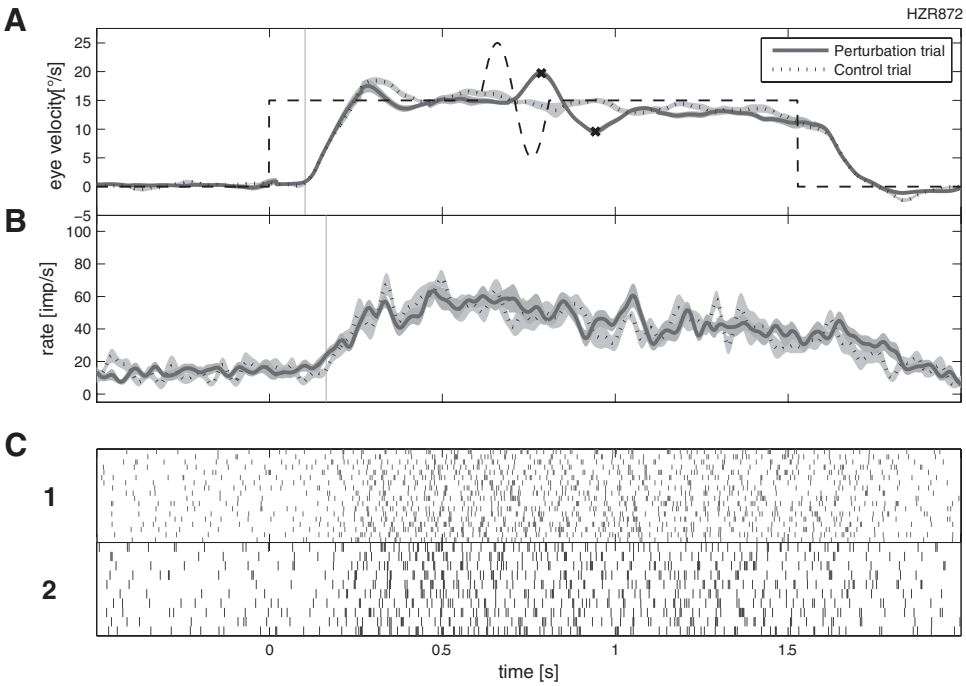

FIG. 3. MSTd neuron, which is modulated during SPEM, but not in relation to eye-movement perturbation. For further explanation see Fig. 1.

perturbation were contaminated by saccades that led to the elimination of these trials. The underlying constant eye velocity during ramp stimulation had a clear effect on the perturbation response in terms of both latency and response modulation (Fig. 4, *A* and *B*).

The mean latency (PRL; see Fig. 1) monotonically decreased from 121 ms at 5°/s ramp velocity to 94 ms at 20°/s ramp velocity. This decrease was highly significant [one-way ANOVA, four levels corresponding to four target velocities: $F(3,158) = 14.99$; $P < 0.0001$] and different from the latency pattern seen in response to the standard step-ramp stimulation. Here stimulus velocity had little effect on latency (see following text; Fig. 4*C*).

In contrast to perturbation latency, the magnitude of the perturbation response (PRM; see Fig. 1) continuously increased from 6.3°/s at 5°/s ramp velocity to 9.3°/s at 20°/s ramp velocity (Fig. 4*B*). This increase was also highly significant [one-way ANOVA, four levels corresponding to four target velocities: $F(3,158) = 12.29$; $P = < 0.0001$]. Both latency and magnitude reflect dynamic gain control with values similar to those described previously (Churchland and Lisberger 2005a).

NEURONAL RESPONSE. Based on the criteria described earlier (METHODS) 22 of 61 neurons (36%) showed some modulation during perturbation, whereas most neurons (64%; HZ, $n = 31$; UJ, $n = 6$; OY, $n = 2$) were not modulated.

A modulated neuron is shown in Fig. 2. Neuronal activity during SPEM started 150 ms after eye movement onset (260 ms after stimulus onset). After a modest phasic response associated with eye acceleration the remaining response was related to eye velocity. The perturbation during pursuit led to an eye-movement response after 121 ms, which was followed 100 ms later by a modulation in neuronal activity (Fig. 2). This sequence of events was the case in virtually all instances. The neuronal activity followed the eye-movement perturbation response on average by 101.6 ms (SD = ±46.1 ms) (Fig. 5*A*). This latency was slightly shorter than the onset of neuronal activity for step-ramp stimulation of the same trials (average

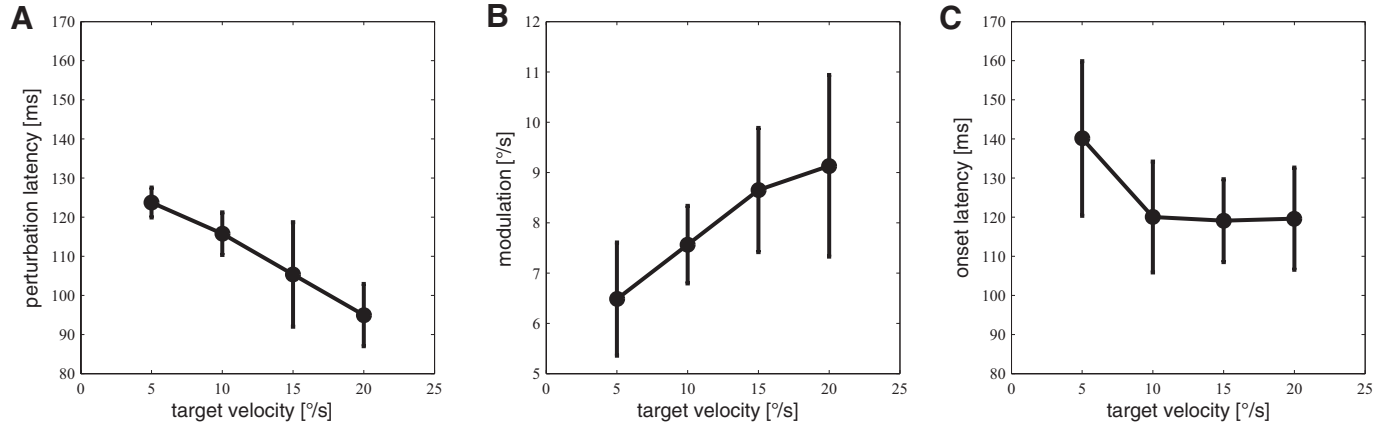

FIG. 4. Perturbation eye-movement latency (*A*) and modulation (*B*) at different underlying constant (ramp) velocities. Increasing ramp velocities lead to a significant decrease in latency and an increase in modulation (gain), which reflects dynamic gain control. *C*: the eye-movement latency to step-ramp stimulation with little effect of target velocity. Vertical lines: SD.

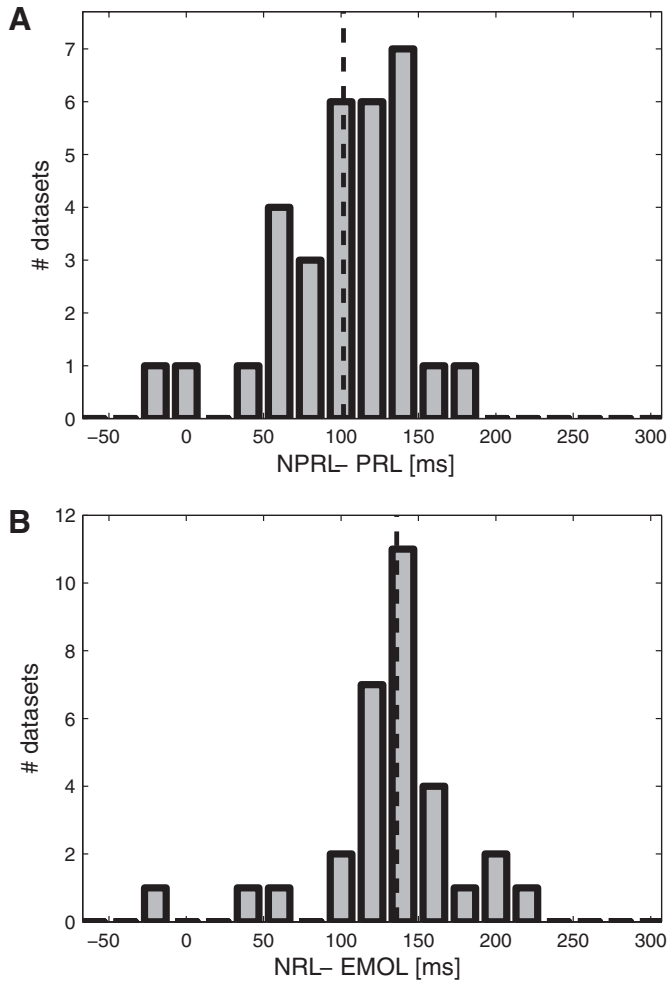

FIG. 5. Neuronal perturbation response latency (NPRL) relative to ocular perturbation response latency (PRL) (*A*) and for the same data sets neuronal response latency after step-ramp target onset (NRL) relative to eye-movement onset latency (EMOL) (*B*). One data set is the neuronal response at a given stimulus velocity. In *A* and *B* neuronal activity starts on average >100 ms after the eye movement. Stippled lines in *A* and *B* show average values.

127.3; SD = ±55.5 ms) (Fig. 5*B*). The mean perturbation latency (NPRL − PRL) decreased with target velocity from 118 ms at 5°/s to 67 ms at 20°/s (Fig. 6*B*). However, this decrease was not significant [one-way ANOVA, four levels corresponding to four target velocities: $F(3,27) = 1.06$; $P = 0.381$]. In general neurons were tested at more than one stimulus velocity, yielding 61 data sets for these 22 neurons. (The term "data set" refers to the neuronal response at one stimulus velocity.) Whereas 6 neurons (HZ, $n = 6$; UJ, $n = 0$; OY, $n = 0$) were modulated under all conditions ($n = 9$), the remaining 16 neurons (HZ, $n = 11$; UJ, $n = 1$; OY, $n = 4$) were not modulated at all stimulus velocities (modulation in 22 of 55 conditions).

As mentioned earlier, most neurons ($n = 39$) did not respond to perturbation at any stimulus velocity (131 conditions). For the example shown in Fig. 3, target perturbation leads to a clear eye-movement modulation (Fig. 3*A*), but not to a modulation of neuronal activity (Fig. 3*B*). Thus although the perturbation led consistently to an eye-movement modulation, most MSTd neurons were not affected.

SPEM step-ramp responses

EYE MOVEMENTS. After the step the eyes started to move with a latency of 120–140 ms with little effect of stimulus velocity (Fig. 4*C*). The timing of the step-ramp prevented in nearly all cases an initial catch-up saccade. The final constant velocity was reached after another 200 ms (Figs. 1–3). Constant eye velocity increased with stimulus velocity, with gain values ranging from 0.85 to 0.95, which reflects normal behavior.

NEURONAL RESPONSES. Preferred directions were equally distributed across the tested directions. Neuronal activity started to increase in nearly all instances after the beginning of smooth pursuit. There was only one neuron that started to discharge 28 ms before eye-movement onset. The average latency (NRL − EMOL; see Fig. 1) for all MSTd neurons ranged from 151 ms at 10°/s to 135 ms at 20°/s target velocity (Fig. 6*A*). Thus there was a small, but not significant effect of stimulus velocity on neuronal latency [one-way ANOVA, four levels corresponding to four target velocities: $F(3,158) = 2.55$; $P = 0.058$]. We found that 75% of the neurons had activity increases, which started >120 ms after stimulus onset. The distribution of latencies for those neurons, in which the perturbation led to neuronal activity changes (Fig. 5*B*), was not different from the nonresponding neurons. During the constant-velocity period activity increased with eye velocity. However, the average sensitivity in relation to eye velocity remained nearly constant.

Relationship between neuronal step-ramp and perturbation responses

With respect to neuronal response latency (NRL), there was no difference between modulated and unmodulated MSTd neurons during perturbation. Responding neurons did not appear to be clustered in certain regions of MSTd. The ratio of phasic (initial) to tonic (constant-velocity) activity was on average slightly higher for the responsive (1.96) than that for the unresponsive (1.71) neurons. Also the constant-velocity sensitivity was slightly higher (3.11 impulses$\cdot s^{-1}\cdot deg^{-1}\cdot s^{-1}$) for responsive neurons compared with 2.46 impulses$\cdot s^{-1}\cdot deg^{-1}\cdot s^{-1}$ for unresponsive neurons (average). Both differences did not become significant (relation phasic vs. tonic: $P = 0.090$, constant-velocity sensitivity: $P = 0.081$; Student's *t*-test). However, although the difference in neuronal sensitivity was modest, it turned out to be critical for understanding why only some neurons had clear responses to the perturbation (see following text).

As shown earlier, the eye-movement perturbation response modulation (PRM) increased with higher constant velocities (Fig. 4*B*). This modulation, however, was not reflected in more responsive data sets at higher stimulus velocities. In contrast, the percentage of responsive data sets decreased with stimulus velocity. Whereas 33% of the data sets were responsive at 5°/s, this number decreased to 23% (10°/s), 21% (15°/s), and 9% (3 of 32) at 20°/s stimulus velocity. This initially surprising finding was also seen with our regression analysis (see following text).

To further investigate why neurons did not show detectable modulation in response to target perturbation, we predicted the neuronal responses in perturbation trials based on the averaged control trials using a linear regression approach (see METHODS). We

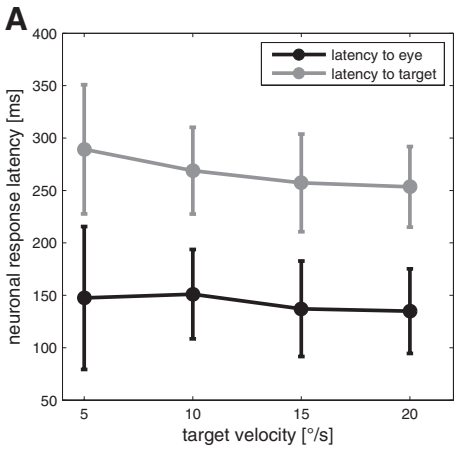

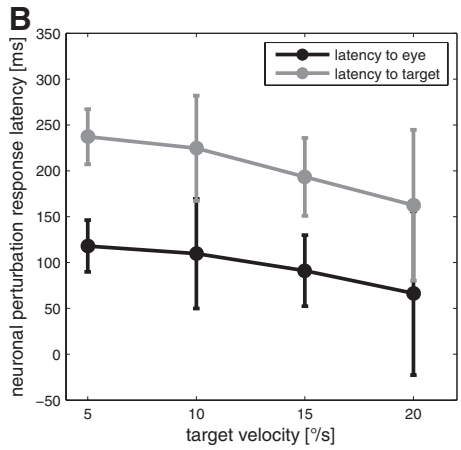

FIG. 6. The effect of target velocity on neuronal latency (*A*) and neuronal perturbation response latency (*B*). Gray: latency to target onset, equivalent to NRL (*A*) and NPRL (*B*), respectively; black: latency relative to eye-movement onset, equivalent to NRL − EMOL (*A*) and NPRL − PRL (*B*), respectively. In *A* target velocity has little effect on neuronal latencies. Neurons are lagging target onset by 250–300 ms. In *B*, both neuronal perturbation response latency with respect to eye and target onset show a small but not significant decrease.

first fitted the neuronal responses in control trials using a combination of eye velocity and eye acceleration. In general, this regression approach provided a good fit of the neural response during control trials, with an average R^2 value of 0.61 ± 0.20 (see Fig. 7 for examples of a responsive and a nonresponsive neuron). Furthermore, the fit of the neuronal control data confirmed that the MSTd neurons basically encode eye velocity with a small eye acceleration component (velocity factor: 2.4 ± 1.6 impulses·s^{-1}·deg^{-1}·s^{-1}; acceleration factor: 0.06 ± 0.16 impulse·s^{-1}·deg^{-1}·s^{-2}). For 64% of the data sets the acceleration component was negligible (<0.001 impulse·s^{-1}·deg^{-1}·s^{-2}). Adding a mixed term (velocity × acceleration) improved the average R^2 to only 0.63 and was therefore not used.

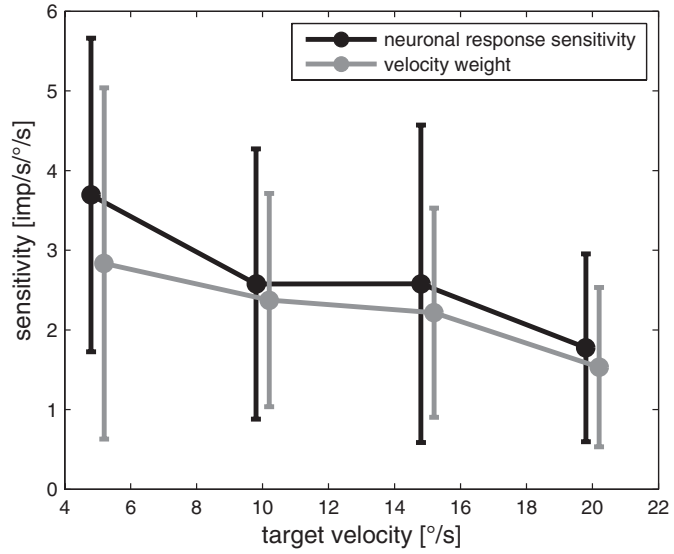

FIG. 7. Prediction of neuronal response to target perturbation. Dashed curve in *A1* shows the averaged neuronal response during a control trial of an MSTd neuron that shows modulation to target perturbation (*A2*). The stippled curve illustrates the result of a curve fitting using a weighted combination of eye velocity, acceleration, and a constant part. The estimated parameters of that regression analysis are used to predict a neuronal response to the eye movements of the perturbation trials, plotted in *A2* as a stippled curve. The gray band in the *bottom panel* illustrates the confidence region, which is used to classify the neuronal responses. To decide whether a neuronal response shows modulation to the target perturbation, a confidence region is defined as 3SD around the Gaussian low-pass filtered spike density function of the control trials. When the firing rate of the perturbation trials exceeds this confidence region in a time interval ≤550 ms after start of target perturbation, this neuronal response is declared to show a perturbation response. Furthermore, the averaged neuronal response during a perturbation trial is plotted as dashed line. Here, both measured and predicted neuronal responses leave the confidence region and show modulation to the target perturbation. Accordingly, these examples are classified as "responsive." A "nonresponsive" neuron that does not show modulation to the target perturbation is illustrated in *B*. The measured and predicted neuronal responses do not leave the confidence region (*B2*).

The perturbation analysis of the *predicted* neuronal response, using the same confidence region as that for the measured perturbation data, revealed that for the majority of data sets (68%), prediction and data were in accordance (20% responsive, 48% nonresponsive). For the remaining data, prediction and measurement did not match (prediction: response − measured: no response: 19%; prediction: no response − measured: response: 13%). In other words, our analysis showed that, based on the response properties of the neurons during step-ramp control trials and the eye movement during perturbation trials, for most nonresponsive neurons a detectable perturbation response was not expected, since the noise level in relation to the velocity weight was too high.

The regression analysis also showed that the predicted neuronal responses were related to target velocity. Whereas at 5°/s 63% of the data sets were predicted as responsive, this percentage decreased to 38% at 10°/s, 32% at 15°/s, and 19% at 20°/s. Thus both the measured (see earlier text) and the predicted responsive data sets decreased with target velocity. This result was not due to an increase of the confidence region (noise) in relation to target velocity (5°/s: 45.5 impulses/s; 10°/s: 56.7 impulses/s; 15°/s: 56.3 impulses/s; 20°/s: 49.5 impulses/s). There was also no difference between responsive and nonresponsive data sets. However, the neuronal sensitivity decreased with target velocity, which can be seen for both the neuronal data and the regression analysis (Fig. 8). In both measures the decrease amounts to a factor of 2 and is significant [neuronal response sensitivity: one-way ANOVA, four levels corresponding to four target velocities, $F(3,158) = 5.5636$; $P = 0.0012$; velocity weight: one-way ANOVA, four levels corresponding to four target velocities, $F(3,158) = 3.7794$; $P = 0.0121$]. The decrease was similar for responsive and nonresponsive data sets. On the other hand, the eye movement perturbation response modulation (PRM) increased with a factor of about 1.5 (see Fig. 4*B*). Thus the effect of decreas-

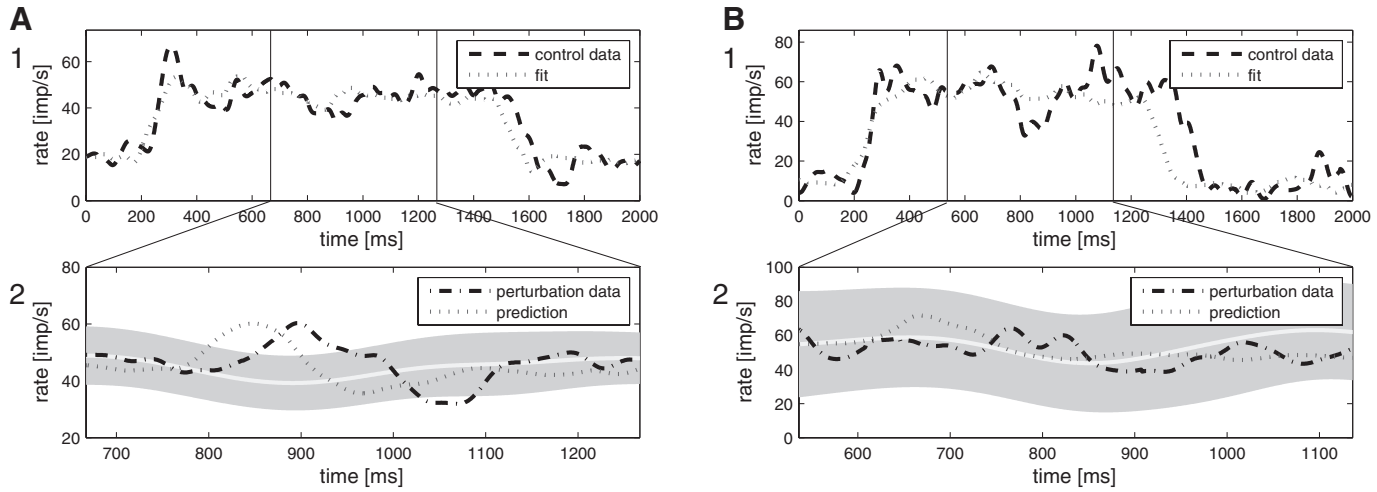

FIG. 8. Dependence of neuronal response sensitivity (black) and regression weight for eye velocity (gray) on target velocity. Both measures decrease with increasing target velocity by a factor of 2. Compare with Fig. 4*B*, which shows that the eye-movement modulation increases by a factor of only about 1.5.

ing neuronal perturbation response with higher target velocity prevails over the effect of increasing ocular perturbation response, which can explain the lower number of responsive data sets with increasing target velocity.

LF motion responses

The main emphasis of this study is on the neuronal responses during smooth-pursuit perturbation. Since virtually all MSTd neurons responding during SPEM also responded during LF visual motion (in the opposite direction), some examples ($n = 15$) were taken to underline the difference in the response characteristics. Values were taken from neurons tested at 15°/s stimulus velocity ($n = 12$). The remaining neurons were tested at 20°/s ($n = 2$) and 5°/s ($n = 1$) with similar results.

LF perturbation responses

EYE MOVEMENTS ASSOCIATED WITH LF MOTION. The LF stimulus consistently led to changes in eye velocity following the perturbation (Fig. 9). For an underlying stimulus velocity of 15°/s, the perturbation (5 Hz, ±10°/s) response latency (PRL) was 88 ± 7.4 ms, slightly shorter than that during SPEM. The eye-movement response modulation (PRM) with 10.5 ± 2.1°/s (corresponding to a gain of 0.53) was also comparable to the value during SPEM.

NEURONAL RESPONSE. All neurons ($n = 15$), except for one, were clearly modulated by the LF perturbation. The sensitivity ranged from 1.01 to 4.77 impulses·s^{-1}·deg^{-1}·s^{-1} and was on average 2.25 impulses·s^{-1}·deg^{-1}·s^{-1}. In contrast to the late onset of smooth-pursuit perturbation responses, neuronal activity following LF motion led the eye-movement response (NPRL, Fig. 9) by 34.1 ms for most neurons (12 of 15). For

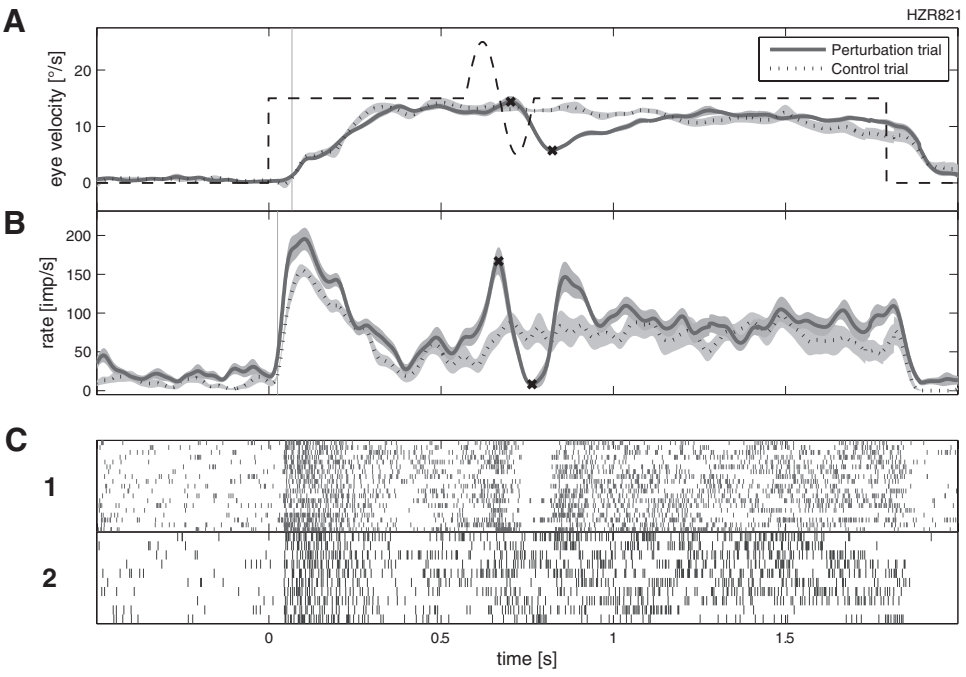

FIG. 9. Response of an MSTd neuron to large-field (LF) visual motion with (straight line) and without (dotted line, control) perturbation. For further details see Figs. 1 and 2. During LF stimulation and perturbation the neuronal response starts before the eye movements.

two neurons activity lagged both for ramp (see following text) and for perturbation. The remaining neuron lagged only during perturbation.

LF ramp responses

EYE MOVEMENTS. The LF stimulus induced eye movements with a latency (EMOL) of 76 ± 20.1 ms, which was much shorter than the 120 ms obtained during SPEM stimulation. Eye velocity at 200 ms poststimulus onset reached 12.3°/s (average) with a 15°/s stimulus.

NEURONAL RESPONSES. In general the neuronal response latency during ramp stimulation (NRL) was short (Fig. 9) except for two neurons with a latency of 209 and 241 ms after stimulus onset. All other neurons (including those tested at 5 and 20°/s) had short latencies (average 42 ± 14 ms) with respect to stimulus onset and started on average 34 ms before the eye movement. This is in sharp contrast to the SPEM situation, during which the neurons responded on average 135 ms following the eye-movement onset.

The sensitivity of the neurons tested with LF stimulation was variable. Some neurons ($n = 4$ of 12) had small steady-state responses (<0.5°/s) but a large initial response, which might reflect the different amount of retinal slip during stimulation. The remaining neurons ($n = 8$) had an average sensitivity of 3.19 impulses$\cdot s^{-1}\cdot deg^{-1}\cdot s^{-1}$.

Responses during target blinking

To confirm the dependence of the smooth-pursuit–related response on extraretinal signals, 22 of the SPEM-related neurons were additionally tested during step-ramp stimulation, with the target blinked for 100 ms during ongoing pursuit (Ono and Mustari 2006). For the tested neurons the neuronal activity started 131 ms (average) after pursuit onset (see earlier text). During the target blink the eye movement continued as smooth pursuit with only a small transient decline in velocity. The minimum in eye velocity was reached 215 ms (average) after blink onset. The gain decreased on average to 0.69 compared with the control gain of 0.90 for the population of tested neurons. The neuronal activity was not significantly affected by the blink. The relation of neuronal activity to eye velocity during the blink analysis period was 109% compared with the 100% for the controls—thus even slightly higher than that under control conditions. It is known that neuronal responses related to *visual motion* (e.g., in area MT) show a pronounced activity decrease during the target blink (Newsome et al. 1988). Thus the continuous response during the target blink supports the nonretinal origin of the responses during SPEM.

DISCUSSION

Our study shows that the characteristic changes in eye movement due to dynamic gain control can be easily demonstrated in accordance with earlier studies (Churchland and Lisberger 2005a,b). With higher ongoing SPEM velocities the perturbation response increases and the latency decreases (Fig. 4). In general the perturbation response latency (PRL) appeared shorter than the SPEM onset latency (EMOL) during step-ramp stimulation, although it has to be kept in mind that the methods for determining SPEM (onset) and perturbation (peak-to-peak) latencies were different (see Fig. 1 and METHODS).

Despite prominent eye-movement changes with perturbation, this was only poorly reflected in the SPEM response of MSTd neurons. Our MSTd neurons had a good sensitivity during pursuit, but a perturbation-related response could be detected for only a minority (36%). Even for the modulated neurons, the perturbation response was not detectable at all stimulus velocities. Interestingly the percentage of responsive data sets decreased with higher stimulus velocities (see RESULTS). This most likely seems to be related to the decrease of neuronal sensitivity with increasing stimulus velocity (Fig. 8), which appears to be higher than the increase of the eye-movement perturbation response (PRM, Fig. 4*B*).

For the classification of neurons, the noise level plays an important role. We chose 3SDs to judge whether a neuronal response shows responsiveness. A higher criterion tends to miss weak responses; a lower one might classify noise as a perturbation response. Our subsequent regression analysis showed that for 68% of our data sets the presence or absence of a neuronal perturbation response was a direct consequence of the dynamic properties of the neurons. The large proportion of nonresponsive neurons is thus explained by the fact that the neuronal discharge is mainly determined by eye velocity and, in these neurons, the expected perturbation modulation was too small compared with the noise level. The remaining 32% fall into two categories: for 13% the measured perturbation response was even larger than predicted, which could be explained by the observation that phasic responses were usually underestimated by our regression model. The remaining 19% of the data sets were expected to show a detectable modulation based on the control data, but the measurement failed to reveal the expected perturbation response.

The relatively late onset of the perturbation-related response seems to argue against participation of MSTd neurons in generation of the perturbation response. However, MSTd neurons could provide a signal that carries a delayed efference copy of eye movements (also see the following text), which is needed to reconstruct a signal representing target velocity in space from a similarly delayed retinal slip signal. From earlier studies it is known that onset of the SPEM component of MSTd neurons often starts >100 ms after eye-movement onset (Newsome et al. 1988). In our sample the average delay was 127 ms. Similarly, the perturbation response occurred 102 ms after the eye movement. MSTd could thus monitor the state of the SP system. The highly direction specific nature and SPEM dependence of responses suggest that MSTd neurons could play a role in maintenance of pursuit (Ono and Mustari 2006). A direct involvement of MSTd in dynamic gain control, however, seems unlikely.

Origin of the nonretinal component

Maintenance of SPEM critically depends on feedback mechanisms providing information about eye velocity (Krauzlis and Lisberger 1994; Nuding et al. 2008; Robinson et al. 1988). One possible source could be the thalamus, where SPEM-related activity has recently been encountered (Tanaka 2005). Here, neuronal activity lags SPEM initiation on average by 30 ms, which is still considerably shorter than the 100–130 ms encountered for our MSTd neurons and found in earlier studies (Newsome et al. 1988). MSTd also receives an input from FEF

(Tusa and Ungerleider 1988), where SPEM-related activity is present as well. Neuronal activity in FEF typically leads SPEM (Tanaka and Fukushima 1998), but there are late-responding neurons, which could account for the delay seen in MSTd.

Recently eye-position–related activity has been discovered in the somatosensory cortex, probably reflecting proprioception (Wang et al. 2007). Although these signals have an average delay of 80 ms after saccade onset (Zhang et al. 2008), they are not appropriate, since MSTd neurons encode gaze rather than eye velocity (Ono and Mustari 2006). Thus the thalamic signal seems adequate, although an explanation is missing as to how the long delay seen in MSTd neurons is generated.

Where does the dynamic gain control take place?

Current studies show that at least two cortical structures are involved in the generation and control of SPEM. Evidence exists to show that the FEF participates more in SPEM initiation and MST more in SPEM maintenance (Nuding et al. 2008), but the roles of these areas and their pontine target areas are not completely separated. Several studies point toward a prominent role of FEF in dynamic gain control. For example, electrical stimulation in FEF enhances a perturbation response (Tanaka and Lisberger 2001). Recently it was shown using transcranial magnetic stimulation (TMS) in humans that the FEF is directly involved in dynamic gain control during SPEM (Nuding et al. 2008). Potentially, dynamic gain control could be the result of some interaction between FEF and MST. However, our data do not support a role for MSTd in such interaction. The MSTd smooth-pursuit signals are too late to allow a substantial contribution to the very reliable eye-movement signals as a result of dynamic gain control. Similar conclusions were drawn in an earlier study (Churchland and Lisberger 2005b) that did not directly investigate neuronal activity during perturbation. Currently, it cannot be excluded that the dynamic gain control results from interaction with other parietooccipital areas, such as MT or MSTl, which so far have not been thoroughly investigated with this question in mind. However, it also seems quite possible that the dynamic gain control results from some local interactions within FEF, where not only SPEM-related but also visual responses are encountered (Fukushima et al. 2002). Alternatively, short-latency visual and eye motion signals in cortical-ponto-cerebellar circuits might all contribute to dynamic gain control.

What is the functional meaning of the extraretinal component of MSTd neurons?

Before considering this question, it has to be emphasized that virtually all MSTd neurons possess large visual-motion–sensitive receptive fields. Importantly, the large majority of neurons has opposite preferred directions for visual and nonretinal components, as described previously (Newsome et al. 1988; Shenoy et al. 2002). In our study LF visual motion induced an OKR response with a short latency (average 76 ms) and the perturbation response during OKR showed a similar latency (average 88 ms). For virtually all neurons LF visual motion and perturbation were accompanied by neuronal activity changes. In contrast to the extraretinal pursuit component, these activity changes occurred much earlier before the eye movement for both ramp and perturbation stimulation (average lead: 34 ms). This general pattern leads to a number of interpretations.

Several studies have put forward the suggestion that extraretinal signals play an important role in pursuit maintenance (Newsome et al. 1988; Nuding et al. 2008; Ono et al. 2009). This is quite plausible despite the large delay of the extraretinal component in MSTd neurons. Interestingly, this neuronal delay (127 ms) and the delay of pursuit onset with respect to target motion (120–140 ms) exhibit similar values. The similarity of temporal delays together with simulations of our nonlinear pursuit model incorporating delays (Brostek et al. 2009) suggest that the extraretinal pursuit signal of MSTd neurons may serve to reconstruct target velocity in space, which then could be represented in MSTl, as suggested previously (Ilg and Thier 2003). The representation of the perturbation response in our MSTd neurons is compatible with this idea, since it reflects what was predicted from our modeling of the step-ramp responses.

One important argument against this hypothesis is that MSTd responses found during LF visual motion do not reflect delayed eye velocity. Thus other roles for the extraretinal signals have to be considered. For example, MST has been shown to be involved in decoding movement through the environment (Duffy and Wurtz 1991). It is thus possible that late-responding MSTd pursuit neurons might be involved in spatial orientation and navigation (Chen et al. 2008). Based on these ideas, a possible hypothesis for the signal coded by our MSTd neurons is that they represent gaze velocity in a spatial reference frame, given that large-field visual motion may be interpreted as self-motion at the processing stage of MSTd.

Ocular following

There have been a number of studies relating MSTd activity to the generation of ocular following. With LF visual motion ocular following occurs 55–60 ms after stimulus onset (Miles et al. 1986). Visual MSTd activity recorded under these conditions started before the eye movements (Kawano et al. 1994). It has been concluded that this visual signal is transferred to the brain stem and the cerebellum to generate the eye-movement response (Kawano 1999). In our study LF visual motion led to comparable results. However, since most MSTd neurons with an extraretinal signal have a preferred direction opposite to the visual response, it appears unlikely that the response of these neurons is used only to drive the ocular following response. Although parietooccipital lesions including MSTd affect the ocular following response (Takemura et al. 2007), specific regions of MST may serve different functions.

Optic flow

Recent reports focus on the responses of MSTd neurons to optic flow (Britten 2008; Shenoy et al. 2002). Furthermore, at least some MSTd neurons compensate for pursuit speed during optic flow, which provides critical information for the computation of self-motion (Shenoy et al. 2002). The authors in this study also determined the smooth-pursuit response of the MSTd neurons, which—as it is known from previous studies—had a preferred direction opposite to the optimal laminar flow direction.

Interestingly, Inaba et al. (2007) found that the visual motion response of MSTd neurons is affected by smooth pursuit even if the neurons do not respond during smooth pursuit per se. This applied to >70% of the MSTd neurons tested. These results also support a role of MSTd in self-motion perception.

Conclusions

Only a minority of smooth-pursuit–related MSTd neurons show detectable modulation in response to short perturbations of the visual stimulus. The responding neurons were modulated on average >100 ms after the eye movement. The small number of responsive neurons can be explained by the discharge properties of MSTd neurons derived from step-ramp responses. Based on these findings it is unlikely that MSTd neurons play a significant role in dynamic gain control. However, the SPEM and perturbation results are still compatible with models, in which MSTd is involved in smooth-pursuit maintenance (Dicke and Thier 1999; Nuding et al. 2008).

If one takes into account that virtually all MSTd neurons with extraretinal signals encode gaze velocity, have large-field motion-sensitive receptive fields, and show visual responses with opposite preferred directions, other functional interpretations have to be considered. In accordance with earlier studies (Shenoy et al. 1999) LF motion could be interpreted as being caused by self-motion in space. Accordingly, SPEM-responsive MSTd neurons could then represent gaze velocity in a spatial reference frame.

GRANTS

This work was supported by National Institutes of Health Grants EY-013308 and RR-00166 and Bernstein Center for Computational Neuroscience Grant BMBF 011GQ0440.

REFERENCES

Britten KH. Mechanisms of self-motion perception. *Annu Rev Neurosci* 31: 389–410, 2008.

Brostek L, Ono S, Mustari MJ, Nuding U, Büttner U, Glasauer S. Neuronal responses in the cortical area MSTd during smooth pursuit and ocular following eye movements. *BMC Neurosci* 10, *Suppl.* 1: P367, 2009.

Büttner U, Büttner-Ennever JA. Present concepts of oculomotor organization. *Prog Brain Res* 151: 1–42, 2006.

Chen CW, Gu Y, Takahashi K, Angelaki DE, DeAngelis GC. Clustering of self-motion selectivity and visual response properties in macaque area MSTd. *J Neurophysiol* 100: 2669–2683, 2008.

Churchland AK, Lisberger SG. Gain control in human smooth-pursuit eye movements. *J Neurophysiol* 87: 2936–2945, 2002.

Churchland AK, Lisberger SG. Discharge properties of MST neurons that project to the frontal pursuit area in macaque monkeys. *J Neurophysiol* 94: 1084–1090, 2005a.

Churchland AK, Lisberger SG. Relationship between extraretinal component of firing rate and eye speed in area MST of macaque monkeys. *J Neurophysiol* 94: 2416–2426, 2005b.

Dicke PW, Thier P. The role of cortical areas MST in a model of combined smooth eye-head pursuit. *Biol Cybern* 80: 71–84, 1999.

Distler C, Mustari MJ, Hoffmann KP. Cortical projections to the nucleus of the optic tract and dorsal terminal nucleus and to the dorsolateral pontine nucleus in macaques: a dual retrograde tracing study. *J Comp Neurol* 444: 144–158, 2002.

Duffy CJ, Wurtz RH. Sensitivity of MST neurons to optic flow stimuli. I. A continuum of response selectivity to large-field stimuli. *J Neurophysiol* 65: 1329–1345, 1991.

Fuchs AF, Robinson DA. A method for measuring horizontal and vertical eye movement chronically in the monkey. *J Appl Physiol* 21: 1068–1070, 1966.

Fukushima K, Yamanobe T, Shinmei Y, Fukushima J. Predictive responses of periarcuate pursuit neurons to visual target motion. *Exp Brain Res* 145: 104–120, 2002.

Ilg UJ, Thier P. Visual tracking neurons in primate area MST are activated by smooth-pursuit eye movements of an "imaginary" target. *J Neurophysiol* 90: 1489–1502, 2003.

Inaba N, Shinomoto S, Yamane S, Takemura A, Kawano K. MST neurons code for visual motion in space independent of pursuit eye movements. *J Neurophysiol* 97: 3473–3483, 2007.

Judge SJ, Richmond BJ, Chu FC. Implantation of magnetic search coils for measurement of eye position: an improved method. *Vision Res* 20: 535–538, 1980.

Kawano K. Ocular tracking: behavior and neurophysiology. *Curr Opin Neurobiol* 9: 467–473, 1999.

Kawano K, Shidara M, Watanabe Y, Yamane S. Neural activity in cortical area MST of alert monkey during ocular following responses. *J Neurophysiol* 71: 2305–2323, 1994.

Komatsu H, Wurtz RH. Relation of cortical areas MT and MST to pursuit eye movements. I. Localization and visual properties of neurons. *J Neurophysiol* 60: 580–603, 1988.

Krauzlis RJ. Recasting the smooth pursuit eye movement system. *J Neurophysiol* 91: 591–603, 2004.

Krauzlis RJ, Lisberger SG. Temporal properties of visual motion signals for the initiation of smooth pursuit eye movements in monkeys. *J Neurophysiol* 72: 150–162, 1994.

Ladda J, Eggert T, Glasauer S, Straube A. Velocity scaling of cue-induced smooth pursuit acceleration obeys constraints of natural motion. *Exp Brain Res* 182: 343–356, 2007.

Leigh RJ, Zee DS. *The Neurology of Eye Movements*. New York: Oxford Univ. Press, 2006.

Maunsell JHR, Van Essen DC. The connections of the middle temporal visual area (MT) and their relationship to a cortical hierarchy in the macaque monkey. *J Neurosci* 3: 2563–2586, 1983.

Miles FA, Kawano K, Optican LM. Short-latency ocular following responses of monkey. I. Dependence on temporospatial properties of visual input. *J Neurophysiol* 56: 1321–1354, 1986.

Mustari MJ, Fuchs AF, Kaneko CRS, Robinson FR, Kaneko CR. Anatomical connections of the primate pretectal nucleus of the optic tract. *J Comp Neurol* 349: 111–128, 1994.

Mustari MJ, Fuchs AF, Wallman J. Smooth-pursuit-related units in the dorsolateral pons of the rhesus macaque. *J Neurophysiol* 60: 664–686, 1988.

Newsome WT, Wurtz RH, Komatsu H. Relation of cortical areas MT and MST to pursuit eye movements. II. Differentiation of retinal from extraretinal inputs. *J Neurophysiol* 60: 604–620, 1988.

Nuding U, Ono S, Mustari MJ, Büttner U, Glasauer S. A theory of the dual pathways for smooth pursuit based on dynamic gain control. *J Neurophysiol* 99: 2798–2808, 2008.

Ono S, Das VE, Mustari MJ. Gaze-related response properties of DLPN and NRTP neurons in the rhesus macaque. *J Neurophysiol* 91: 2484–2500, 2004.

Ono S, Mustari MJ. Extraretinal signals in MSTd neurons related to volitional smooth pursuit. *J Neurophysiol* 96: 2819–2825, 2006.

Ono S, Mustari MJ. Smooth pursuit-related information processing in frontal eye field neurons that project to the NRTP. *Cereb Cortex* 19: 1186–1197, 2009.

Rashbass C. The relationship between saccade and smooth tracking eye movements. *J Physiol* 159: 326–338, 1961.

Robinson DA, Gordon JL, Gordon SE. A model of the smooth pursuit eye movement system. *Biol Cybern* 55: 43–57, 1988.

Schwartz JD, Lisberger SG. Initial tracking conditions modulate the gain of visuo-motor transmission for smooth pursuit eye movements in monkeys. *Vis Neurosci* 11: 411–424, 1994.

Shenoy KV, Bradley DC, Andersen RA. Influence of gaze rotation on the visual response of primate MSTd neurons. *J Neurophysiol* 81: 2764–2786, 1999.

Shenoy KV, Crowell JA, Andersen RA. Pursuit speed compensation in cortical area MSTd. *J Neurophysiol* 88: 2630–2647, 2002.

Suzuki DA, Yamada T, Yee RD. Smooth-pursuit eye-movement-related neuronal activity in macaque nucleus reticularis tegmenti pontis. *J Neurophysiol* 89: 2146–2158, 2003.

Takemura A, Murata Y, Kawano K, Miles FA. Deficits in short-latency tracking eye movements after chemical lesions in monkey cortical areas MT and MST. *J Neurosci* 27: 529–541, 2007.

Tanaka M. Involvement of the central thalamus in the control of smooth pursuit eye movements. *J Neurosci* 25: 5866–5876, 2005.

Tanaka M, Fukushima K. Neuronal responses related to smooth pursuit eye movements in the periarcuate cortical area of monkeys. *J Neurophysiol* 80: 28–47, 1998.

Tanaka M, Lisberger SG. Regulation of the gain of visually guided smooth-pursuit eye movements by frontal cortex. *Nature* 409: 191–194, 2001.

Thier P, Koehler W, Buettner UW. Neuronal activity in the dorsolateral pontine nucleus of the alert monkey modulated by visual stimuli and eye movements. *Exp Brain Res* 70: 496–512, 1988.

Tusa RJ, Ungerleider L. Fiber pathways of cortical areas mediating smooth pursuit eye movements in monkeys. *Annu Rev Neurosci* 23: 174–183, 1988.

Wang X, Zhang M, Cohen IS, Goldberg ME. The proprioceptive representation of eye position in monkey primary somatosensory cortex. *Nat Neurosci* 10: 640–646, 2007.

Zhang M, Wang X, Goldberg ME. Monkey primary somatosensory cortex has a proprioceptive representation of eye position. *Prog Brain Res* 171: 37–45, 2008.